IEEE Photonics Journal
An IEEE Photonics Society Publication

Open Access

Photonic Crystal Fiber in Photonic Crystal Fiber for Residual Dispersion Compensation Over E + S + C + L + U Wavelength Bands

Volume 5, Number 3, June 2013

D. C. Tee
M. H. Abu Bakar
N. Tamchek
F. R. Mahamd Adikan

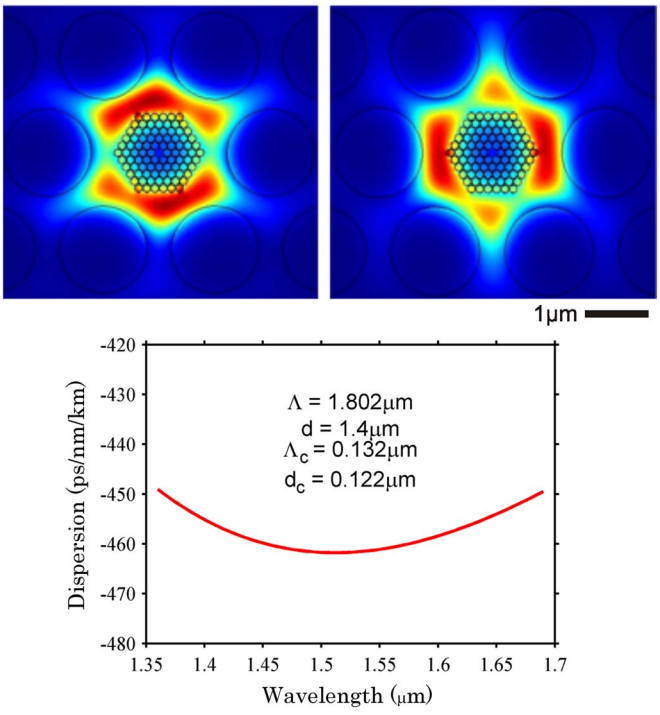

DOI: 10.1109/JPHOT.2013.2265980
1943-0655/$31.00 ©2013 IEEE

IEEE photonics SOCIETY

IEEE

Photonic Crystal Fiber in Photonic Crystal Fiber for Residual Dispersion Compensation Over E + S + C + L + U Wavelength Bands

D. C. Tee,[1] M. H. Abu Bakar,[2] N. Tamchek,[3] and F. R. Mahamd Adikan[1]

[1]Photonics Research Group, Department of Electrical Engineering, Faculty of Engineering, University of Malaya, Kuala Lumpur 50603, Malaysia
[2]Wireless and Photonics Networks Research Center, Faculty of Engineering, University Putra Malaysia, Serdang 43400, Malaysia
[3]Department of Physics, Faculty of Science, University Putra Malaysia, Serdang 43400, Malaysia

DOI: 10.1109/JPHOT.2013.2265980
1943-0655/$31.00 ©2013 IEEE

Manuscript received April 8, 2013; revised May 19, 2013; accepted May 24, 2013. Date of current version June 11, 2013. This work is supported in part by the Ministry of Higher Education, Malaysia, under High Impact Research Grant A000007-50001 and in part by the University of Malaya under the PPP (PV137-2012A) research grant. Corresponding author: D. C. Tee (e-mail: tdchai123@gmail.com).

Abstract: A photonic crystal fiber in photonic crystal fiber (PCF-in-PCF) architecture is numerically investigated for residual dispersion compensation in optical transmission link. The optimized structure shows a flattened and high average dispersion of −457.4 ps/nm/km in the wavelength range of 1360 nm to 1690 nm. The sensitivity of the fiber dispersion properties to a ±2% variation in the optimum parameters is studied for practical conditions. Additionally, the effect of variation in the structure parameters on effective mode area is simulated to understand its relationship to light confinement.

Index Terms: Optical-fiber dispersion, photonic crystal fiber (PCF), finite-element methods.

1. Introduction

The use of optical fiber in communication has revolutionized the telecommunication industry in the way signal is transmitted. The application of optical fiber in long haul transmission requires small but nonzero chromatic dispersion fiber to avoid nonlinear interaction that will cause signal distortion [1]. Standard single-mode fiber has positive chromatic dispersion that leads to greater dispersion magnitude as the optical signal travels over longer distances. Therefore, a dispersion management system has to be designed to nullify the accumulated positive dispersion in order to ensure signal integrity. This can be achieved by inserting dispersion-compensating fiber (DCF) with negative dispersion in the transmission link [2], [3]. Unfortunately, there is always residual dispersion that remains even after the DCF, thus requiring additional dispersion compensation.

Photonic crystal fiber (PCF), with periodic arrangement of air holes running along the longitudinal direction, shows many interesting characteristics unachievable by conventional optical fiber. By tuning the air holes or with special transverse structure design, the dispersion can be tailored to complement the weakness of optical systems. With this in mind, PCF with large flattened negative dispersion was proposed by many researchers to address the residual dispersion issue. An ultra-flattened negative dispersion PCF with average dispersion of −98.3 ps/nm/km and absolute variation (ΔD) of ∼1.1 ps/nm/km over 1480 nm–1630 nm was reported in [4]. The design by

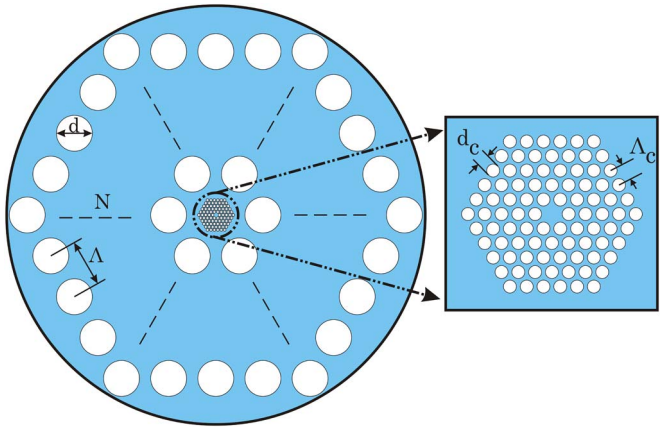

Fig. 1. Transverse cross section of the proposed PCF-in-PCF structure.

Franco *et al.* [5] shows higher average dispersion of -179 ps/nm/km and ΔD around $\sim$2.1 ps/nm/km over wider bandwidth from S- to U-band. In general, both the designs have limited wavelength bands and low negative dispersion, which restricted their application as efficient residual dispersion compensator. Later, a high negative dispersion of -212 ps/nm/km and ΔD of $\sim$11 ps/nm/km over E + S + C + L + U wavelength bands was obtained with a Ge-doped core by using genetic algorithm for optimization [6]. More recently, an equiangular-spiral-typed PCF was designed to have average dispersion of -227 ps/nm/km and ΔD of $\sim$11.9 ps/nm/km over the entire E + S + C + L + U wavelength bands [7]. However, this equiangular-spiral-typed PCF is difficult to fabricate by using the conventional stack-and-draw method.

In this paper, we report a numerical investigation on PCF-in-PCF for compensating the residual dispersion following DCF usage. The PCF-in-PCF structure exhibits ultrahigh negative dispersion (-457.4 ps/nm/km) over wavelengths range bigger than E + S + C + L + U (1360 nm to 1690 nm). In addition, the effect of variation in structure parameters on dispersion value and effective mode area is investigated. Finally, we obtained the nonlinear coefficient from the effective-mode-area characteristic.

2. PCF-in-PCF Design

The idea of using PCF-in-PCF comes from the fact that, by using dual-core PCF, an ultrahigh negative dispersion value can be obtained when the signal is coupled from inner core to outer core at phase matching wavelength [8], [9]. A scaled-down PCF is inserted in the core of a conventional PCF to push the light to be confined in between the first air-hole ring of the conventional PCF and the outer-air-hole ring of the scaled-down PCF. Fig. 1 shows the transverse cross section of the proposed structure on the x–y plane. The air holes are arranged in hexagonal lattice with the distance between the outer holes denoted as Λ and outer hole diameter as d. Additionally, the distance between holes in the core region is Λ_c, and diameter of hole in the core is d_c. The value of d_c and Λ_c is simulated to obtain the desired flattened negative dispersion, and at the same time, the size of the inner air holes must be within the range of the reported fabrication dimension for practical purpose [10]. The number of air-hole rings in the core region is chosen to give high negative dispersion value. The air-hole ring number is fixed to $N = 5$ through the variation of the number of inner-air-hole rings, which finally leads to the desired output. On the other hand, the number of air-hole rings at outer region is selected to give low confinement loss [5]. There are seven rings of air holes at the outer region to reduce the confinement loss for the proposed structure.

A commercial full-vectorial finite-element software (COMSOL) was used to evaluate the proposed structure. The simulation region was truncated by utilizing a perfectly matched layer surrounding the

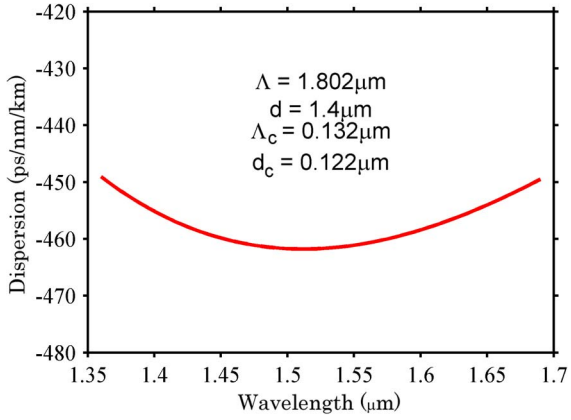

Fig. 2. Flattened negative dispersion over E + S + C + L + U wavelength bands at optimum parameters.

structure. The wavelength-dependent refractive index of the silica was included in the simulation from Sellmeier equation. The chromatic dispersion D was evaluated using

$$D = -\frac{\lambda}{c}\frac{d^2\mathrm{Re}[n_{\mathrm{eff}}]}{d\lambda^2} \tag{1}$$

where c is the velocity of light in vacuum, and $\mathrm{Re}[n_{\mathrm{eff}}]$ is the real part of the effective index. In addition, the effective mode area A_{eff} was calculated with

$$A_{\mathrm{eff}} = \frac{\left(\iint |E^2|\, dx\, dy\right)^2}{\iint |E|^4\, dx\, dy}. \tag{2}$$

3. Numerical Results

Generally, a good residual DCF should have flattened negative dispersion with very high magnitude across the whole wavelength bands of interest. Our proposed PCF-in-PCF design shows a very high average dispersion around -457.4 ps/nm/km with ΔD equal to 12.7 ps/nm/km (range from -449.1 ps/nm/km to -461.8 ps/nm/km) in the wavelength range from 1360 nm to 1690 nm, in which it covers not only the entire E- to U-band but also an additional 15 nm beyond the U-band (see Fig. 2). These characteristics are achieved at the optimum parameters of $\Lambda = 1.802$ μm, $d = 1.4$ μm, $\Lambda_c = 0.132$ μm, and $d_c = 0.122$ μm. The optimum parameters were obtained by simulating many combinations of the aforementioned fiber parameters, and finally, by varying only one of the parameters during each subsequent simulation, the result is converged to the desired output. Compared with the previous best result in the similar wavelength range [7], the proposed structure shows two times higher average dispersion. In addition, this value is eight times higher than the conventional DCF [11]. Such high negative dispersion might be attributed to the dissimilarity of the fundamental guided mode to the typical Gaussian profile of conventional fiber mode. As a result, the proposed fiber is more attractive for practical deployment in dispersion compensation with a shorter fiber length and lower cost compared with the conventional DCF. Fig. 3 shows the time-averaged Poynting vector profile in the propagation direction for both fundamental degenerate modes at 1550-nm wavelength. It can be observed that the modes are confined around the outer region of the inner PCF due to the relatively higher refractive index as compared with the lower refractive index of the subwavelength air holes in the center region.

For fabrication consideration, it is important to evaluate the impact of the changes in structural parameters to the dispersion properties of the proposed structure. Experimental results show that,

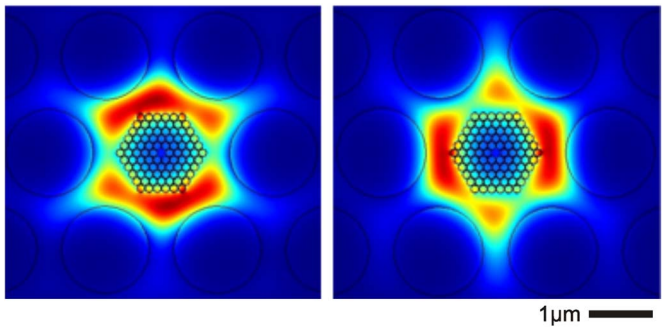

Fig. 3. Time-averaged Poynting vector profile for the two degenerate modes at 1550nm wavelength.

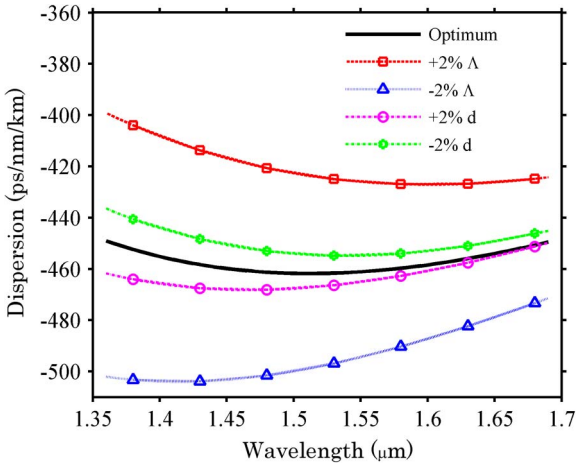

Fig. 4. Sensitivity of the dispersion for $\pm 2\%$ variation in Λ and d. (Seven markers on each dispersion curve are solely for better illustration purpose.)

in PCF fabrication, tolerances in the structural parameters can occur up to $\pm 2\%$ [12]. Therefore, we have numerically studied the effect of $\pm 2\%$ variation in the structural parameters to the average dispersion and absolute dispersion variation. The tolerance analysis is done by changing one parameter at a time while all other optimum parameters are fixed. Fig. 4 shows the sensitivity of the dispersion when a change in $\pm 2\%$ is applied on Λ and d. The changes of the aforementioned two parameters do not significantly alter the shape of the dispersion curve as the guided mode profile demonstrates little variation with adjustments to the outer PCF parameters. A $\pm 2\%$ variation in the Λ causes $\sim \pm 8\%$ changes in the average dispersion while ΔD increases more than 100%, whereas a $\pm 2\%$ deviation in d only affects the average dispersion by $\sim \pm 1\%$ with around 40% increase in ΔD.

In Fig. 5, we demonstrate the effect of $\pm 2\%$ variation on the Λ_c and d_c toward the dispersion characteristics. Visual inspection of the figure exhibits substantial changes to the shape of the dispersion curve with variations in the aforementioned parameters. The changes in the average dispersion over the wavelength bands are less than $\pm 0.5\%$ with an increase of $\sim$70% in ΔD for $\pm 2\%$ variation in Λ_c. As for the case of d_c, a $\pm 2\%$ variation induces $\pm 4\%$ changes in average dispersion, while ΔD is increased by more than 100% and $\sim$20% for $+2\%$ and -2% variations, respectively.

Precise control during the fabrication of the subwavelength air holes in the core region is crucial for the proposed structure. The fabrication of our structure is possible with the assistance of standard stack-and-draw technique [13]. Nowadays, subwavelength air hole with diameter around 110 nm in the core region of silica PCF has been fabricated by standard stack-and-draw technique

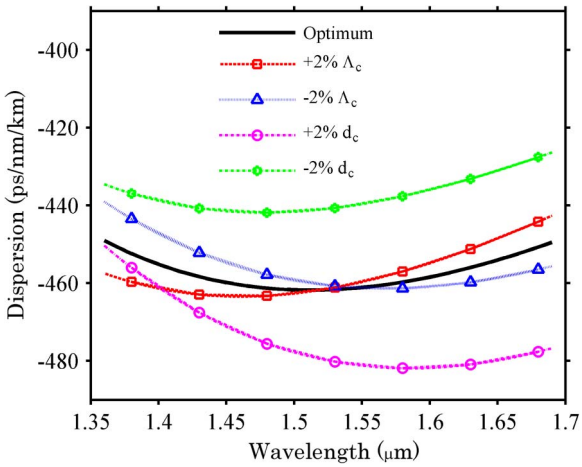

Fig. 5. Sensitivity of the dispersion for $\pm 2\%$ variation in Λ_c and d_c. (Seven markers on each dispersion curve are solely for better illustration purpose.)

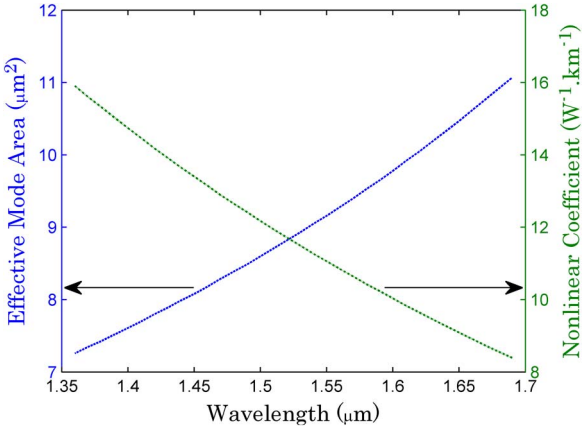

Fig. 6. Effective mode area and nonlinear coefficient as function of wavelength at optimum parameters.

[10]. Since the smallest air-hole size in our proposed structure is 122 nm (which is larger than the fabrication dimension reported in [10]), this ensures that our design can be fabricated using the stack-and-draw technique. Furthermore, air-hole size as small as 20 nm in core region was already achieved in lead silicate PCF by using extrusion technique [14].

The effective mode area as a function of wavelength at optimum parameters is shown in Fig. 6. Since the effective mode area is a quantitative measurement of the area covered by guided mode of the fiber, the width of the guided mode becomes bigger as the operating wavelength increases. Hence, the effective mode area will increase with the longer wavelength. In addition, the corresponding nonlinear coefficient as a function of wavelength is shown in the same figure. The calculated nonlinear coefficient of our structure is around 11.26 $W^{-1} \cdot km^{-1}$ at 1550-nm wavelength under the assumption that the material related nonlinear coefficient is equal to 2.5×10^{-20} $m^2 \cdot W^{-1}$. For optical transmission link, lower nonlinear coefficient from the transmission medium is necessary to reduce unwanted nonlinear effect such as four-wave mixing. Our proposed structure exhibits smaller nonlinear coefficient compared to previous residual dispersion compensator [5]–[7] due to the higher effective mode area.

Fig. 7 shows the variation of effective mode area as a function of d_c/Λ_c at different d/Λ ratio. At fixed value of d/Λ, the effective mode area increases as the ratio of d_c/Λ_c becomes higher. This is due to the fact that the average effective refractive index at the core region is reduced as the d_c

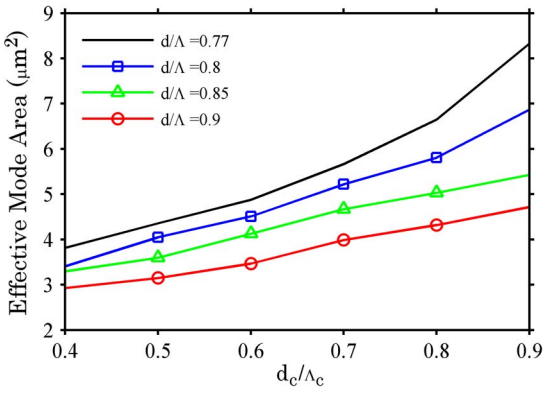

Fig. 7. Variation of effective mode area in function of d_c/Λ_c and d/Λ at fixed inner-air-hole pitch, $\Lambda_c = 0.132$ μm and outer-air-hole pitch, $\Lambda = 1.802$ μm. The black line without markers shows the effect of changing d_c on effective mode area at optimum parameters.

increases. Hence, the light confinement in the core region is weaker since the light is forced out to the cladding region by the inner air holes [15]. Furthermore, the light confinement is better around the core region as the ratio of d/Λ increases. The enlarged size of the air holes at the cladding region prevents the light from dissipating into cladding region and hence increases the light confinement.

Compensation on residual dispersion slope after DCF module is important in the optical-fiber link. The remaining residual dispersion slope is expected to be very small since it has been compensated by DCF. Therefore, small dispersion slope value is needed for residual dispersion compensator. For our proposed structure, the calculated dispersion slope ranges from -0.18 ps/nm^2/km to 0.12 ps/nm^2/km over the 1360-nm-to-1690-nm wavelength at optimum parameters. Over the most widely used S- and C-bands, the dispersion slope range from -0.05 ps/nm^2/km to 0.04 ps/nm^2/km with the most flattened dispersion slope occurring at 1515-nm wavelength, which is equal to 0.0008 ps/nm^2/km.

At 1550-nm wavelength, the absolute birefringence of the structure is around 10^{-7}. This negligible birefringence value is due to the fact that our structure is symmetric; hence, the effective index of the x-polarized and y-polarized fundamental guided modes is degenerated. Compared to [7], which is designed to have high birefringence, negligible birefringence from our proposed structure is more useful in optical transmission link. This is due to the use of circularly symmetric profile similar to standard SMF, which has negligible birefringence value. Hence, compensation of birefringence in transmission link is negligible.

The ability of the structure to guide light with minimum loss was considered by analyzing the confinement loss. The loss can be as low as 0.09 dB/km when N = 10 and even lower when the number of air-hole rings is increased. Besides increasing the number of rings, this loss can be reduced by enlarging the air holes at outer rings [16].

Another loss parameter that has to be considered is the splice loss. Modal field mismatch from the coupling between PCF-based DCF and conventional SMF is the major loss contributing to splice loss. From Fig. 6, the effective mode area is approximately 9 μm^2 at 1550-nm wavelength, and the mode-field diameter is around 3.4 μm. The calculated splice loss of our proposed fiber to a standard SMF with mode-field diameter of 10 μm is found to be 4.3 dB under the condition of zero transverse misalignment between both fibers. With the help of special fusion splicing technique as reported in [17], the splice loss can be further reduced.

4. Conclusion

In conclusion, we have numerically shown that the proposed PCF-in-PCF can be used as a residual-DCF over a bandwidth of 1.36 μm to 1.69 μm. The structure demonstrates an ultrahigh average dispersion of -457.4 ps/nm/km with flattened dispersion between -449.1 ps/nm/km to

-461.8 ps/nm/km over 330-nm wavelength range. Our result is attractive because the achieved average negative dispersion is two times higher than the previous best result [7] and eight times much higher than the conventional DCF [11]. This makes our structure a promising cost effective residual compensator for commercial use. The sensitivity analyses show that the effect of Λ variation is most apparent on average dispersion, while the changes in any parameter will alter the flatness of the dispersion curve. In addition, the effective mode area increases as the wavelength becomes longer and also when the air-hole size increases. At 1550-nm wavelength, the effective mode area is 9 μm^2 with nonlinear coefficient of 11.26 $W^{-1} \cdot km^{-1}$ and splice loss of around 4.3 dB. For future similar work as reported in this paper, the use of common optimization technique such as genetic algorithm method is desirable to achieve optimum parameters in a more systematic approach and to prevent local optimum parameters from occurring. Lastly, with the subwavelength air hole reported in [10], we believe that the fabrication of the structure can be done through standard stacking process [13] to expedite fiber drawing work in the near future.

Acknowledgment

The authors would like to thank W. R. Wong for her technical help.

References

[1] G. P. Agrawal, *Fiber-Optic Communication Systems*, 3rd ed. New York, NY, USA: Wiley, 2002, pp. 15–64.
[2] F. Gerome, J.-L. Auguste, and J.-M. Blondy, "Design of dispersion-compensating fibers based in a dual-concentric-core photonic crystal fiber," *Opt. Lett.*, vol. 29, no. 23, pp. 2725–2727, Dec. 2004.
[3] Y. Liu, J. Wang, Y. Li, R. Wong, J. Li, and X. Xie, "A novel hybrid photonic crystal dispersion compensating fiber with multiple windows," *Opt. Laser Technol.*, vol. 44, no. 7, pp. 2076–2079, Oct. 2012.
[4] S. Varshney, N. Florous, K. Saitoh, M. Koshiba, and T. Fujisawa, "Numerical investigation and optimization of a photonic crystal fiber for simultaneous dispersion compensation over S + C + L wavelength bands," *Opt. Commun.*, vol. 274, no. 1, pp. 74–79, Jun. 2007.
[5] M. A. R. Franco, V. A. Serrão, and F. Sircilli, "Microstructured optical fiber for residual dispersion compensation over S + C + L + U wavelength bands," *IEEE Photon. Technol. Lett.*, vol. 20, no. 9, pp. 751–753, May 2008.
[6] J. P. da Silva, D. S. Bezerra, V. F. Rodriguez-Esquerre, I. E. da Fonseca, and H. E. Hernandez-Figueroa, "Ge-doped defect-core microstructured fiber design by genetic algorithm for residual dispersion compensation," *IEEE Photon. Technol. Lett.*, vol. 22, no. 18, pp. 1337–1339, Sep. 2010.
[7] M. A. Islam and M. S. Alam, "Design of a polarization-maintaining equiangular spiral photonic crystal fiber for residual dispersion compensation over E + S + C + L + U wavelength bands," *IEEE Photon. Technol. Lett.*, vol. 24, no. 11, pp. 930–932, Jun. 2012.
[8] A. Huttunen and P. Torma, "Optimization of dual-core and microstructure fiber geometries for dispersion compensation and large mode area," *Opt. Exp.*, vol. 13, no. 2, pp. 627–635, Jan. 2005.
[9] J. Yuan, X. Sang, C. Yu, C. Jin, X. Shen, G. Zhou, S. Li, and L. Hou, "Large negative dispersion in dual-concentric-core photonic crystal fiber with hybrid cladding structure based on complete leaky mode coupling," *Opt. Commun.*, vol. 284, no. 24, pp. 5847–5852, Dec. 2011.
[10] G. S. Wiederhecker, C. M. B. Cordeiro, F. Couny, F. Benabid, S. A. Maier, J. C. Knight, C. H. B. Cruz, and H. L. Fragnito, "Field enhancement within an optical fibre with a subwavelength air core," *Nat. Photon.*, vol. 1, no. 2, pp. 115–118, 2007.
[11] J. Rathje, M. N. Andersen, and L. G. Nielsen, "Dispersion compensating fiber for identical compensation in the S, C, and L band," in *Proc. OFC*, Mar. 23–28, 2003, vol. 2, pp. 718–719.
[12] F. Poletti, V. Finazzi, T. M. Monro, N. Broderick, V. Tse, and D. J. Richardson, "Inverse design and fabrication tolerances of ultra-flattened dispersion holey fibers," *Opt. Exp.*, vol. 13, no. 10, pp. 3728–3736, May 2005.
[13] J. C. Knight, T. A. Birks, P. St. J. Russell, and D. M. Atkin, "All-silica single-mode optical fiber with photonic crystal cladding," *Opt. Lett.*, vol. 21, no. 19, pp. 1547–1549, Oct. 1996.
[14] Y. Ruan, H. Ebendorff-Heidepriem, V. Afshar, and T. M. Monro, "Light confinement within nanoholes in nanostructured optical fibers," *Opt. Exp.*, vol. 18, no. 25, pp. 26 018–26 026, Dec. 2010.
[15] Y. Ruan, S. Afshar, and T. M. Monro, "Light enhancement within nanoholes in high index contrast nanowires," *IEEE Photon. J.*, vol. 3, no. 1, pp. 130–139, Feb. 2011.
[16] K. Saitoh, M. Koshiba, T. Hasegawa, and E. Sasaoka, "Chromatic dispersion control in photonic crystal fibers: Application to ultra-flattened dispersion," *Opt. Exp.*, vol. 11, no. 8, pp. 843–852, Apr. 2003.
[17] L. Xiao, W. Jin, and M. Demokan, "Fusion splicing small-core photonic crystal fibers and single-mode fibers by repeated arc discharges," *Opt. Lett.*, vol. 32, no. 2, pp. 115–117, Jan. 2007.